Indian Journal of Geo Marine Sciences
Vol. 48 (12), December 2019, pp. 1999-2005

New insights on structure and tectonics over the Laxmi Ridge using EIGEN6C4 modelled gravity data

Ujjawal Kumar, Satya Narayan & S. K. Pal*

Department of Applied Geophysics, Indian Institute of Technology (Indian School of Mines), Dhanbad – 826 004, India
*[E-mail: sanjitism@gmail.com]

Received 27 April 2018; revised 23 July 2018

A comparative analysis has been attempted for the study of structural and tectonic trends over and around (14^0–19^0 N latitudes and 64^0–70^0 E longitudes) the Laxmi ridge. Initially, three different edge enhancement techniques comprising total horizontal derivative (THD), analytical signal (AS) and Theta map have been tested over synthetic prismatic models with varying depths. It is observed that Theta map technique is relatively suitable for delineation of the edges for the sources at different depths. The free-air gravity (FAG) of the Laxmi ridge and surroundings have been generated using EIGEN6C4 high resolution combined earth gravity modelled data. Upward continued gravity anomaly at 20 Km, 40 km, 60 km, 90 km and 150 km heights have been estimated and these are further enhanced using Theta map technique. The enhanced upward continued maps at different height reveal that the sources of the Laxmi ridge low anomaly is constituted by crust, low density upper mantle materials and recent sediments. Present study reveals that the EIGEN6C4 modelled data could be used effectively to identify various structural features of different wavelength. The study reveals that the major lineaments trends are found along N-S, NE-SW and NW-SE directions followed by E-W, ENE-WSW and NNW-SSE directions including different regional and shallow lineaments trends. The delineated lineaments and their orientations are the results of multiple phases of rifting and breakup of India, Madagascar and Seychelles, since its initial stage.

[Keywords: Directional analysis, edge enhancement, EIGEN6C4, Laxmi ridge, lineament mapping, upward continuation,].

Introduction

The evolution of the Western Indian offshore region was due to separation of Madagascar and Seychelles micro-continents from India during the Cretaceous period and the crust_area is characterised as typical volcanic origin[1,2,3]. There are numerous well-known massive structures (Fig. 1) e.g., the Laxmi ridge, the Carlsberg ridge, the Laccadive ridge, the Comorin ridge and the Pratap ridge, which have been identified in the locality of the Western offshore region and are concealed under Indus Fan sediments. Since its evolution, crust of the region has suffered multiple phases of paleogeographic reconstructions and tectonic activities. Several surface / subsurface structural and tectonic features in this region are the consequences of these multi-phase drifting, rifting, magmatic under-plating and seafloor spreading phenomena.

The Laxmi ridge (Fig. 1) is a NW–SE trending structurally high underwater structure, which falls within 14^0–19^0 N latitudes and 64^0–70^0 E longitudes in the Western Indian Offshore. Based on associated gravity low and magnetic anomaly characteristics, it was established that the ridge turns along the WNW–ESE direction from its initial NW–SE direction at around $65^0 30$ E and extends in westwards direction up to $63^0 40$ E[4,5]. It is 0.5 km buried under thick Indus sediments, 100 km wide and 700 km long structure, which run nearly parallel to the west coast of India and topographically rugged in nature[6,7,8,9]. The basement characteristics of the ridge area and its surroundings are uneven and relatively shallower. This may be due to presence of several highs and lows in the area. Gravity anomaly increases from south to north direction over entire study area. The Laxmi ridge is characterized by distinct low gravity (negative) anomalies, which are rarely marked over ocean ridges. Due to negative gravity anomaly behaviours, Laxmi Ridge is regarded as a unique feature in the Western Indian Ocean like the 85^0E ridge in the Bay of Bengal[10]. Even though numbers of investigations have been carried out in the study area, the characteristics of the crust in the region are still ambiguous. Therefore, mapping of structural and deformational trends over the region has become essential due to its economical prospecting in

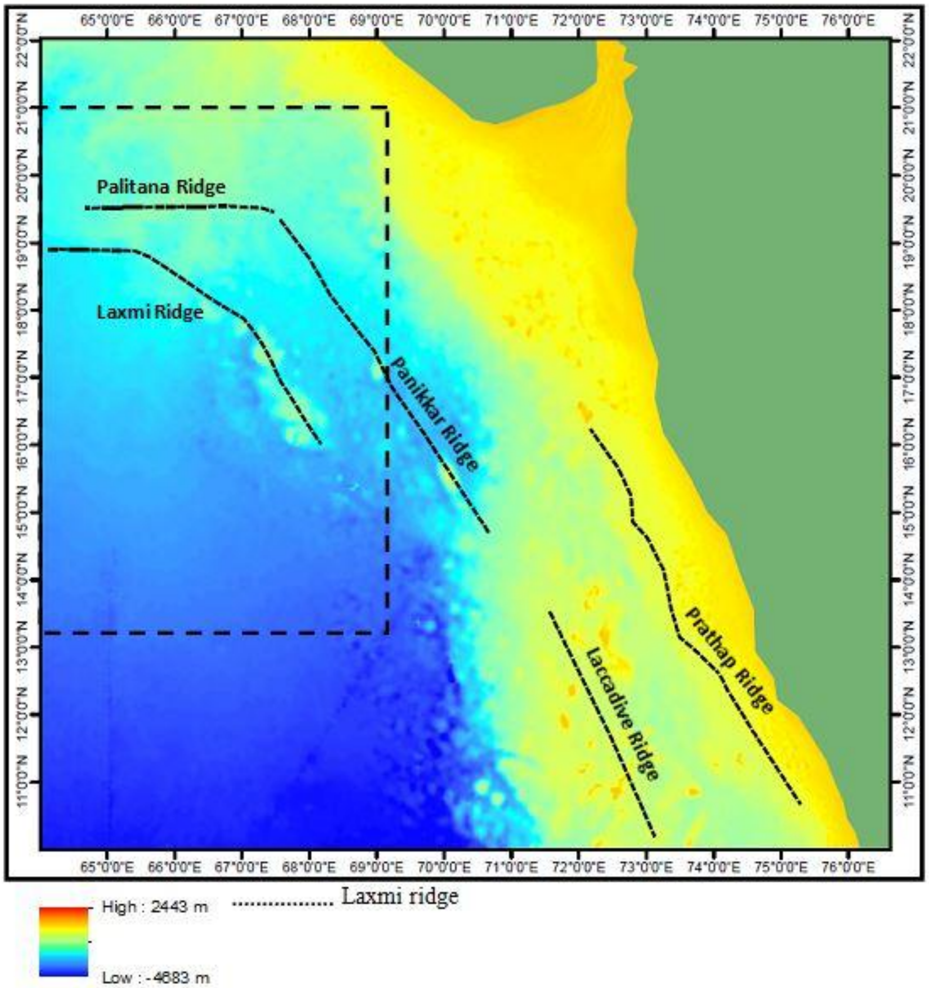

Fig. 1 — Location map showing different ridges marked on the bathymetry. The dashed box indicates the boundary of the study area.

hydrocarbon exploration[11], especially in the offshore regions[12,13]. To have better understanding about the crustal behaviour of the region, it is very important to recognize the depth of anomaly sources, prominent structures, course of tectonic activities and its evolution records using high resolution geophysical data.

EIGEN-6C4 FAG data

In recent past, several global gravity models i.e. EIGEN6C4, EGM2008, EIGEN6S4, GGM05C, GECO etc. have been extensively utilized for the exploration of earth's geological and geodynamical activities particularly in remote and inaccessible areas[14-18]. The EIGEN6C4 is the fourth release of EIGEN6C (European Improved Gravity model of the Earth by New techniques) with maximum degree and order of 2190. It is computed by using LAGEOS (Laser GEOdynamics Satellite), GRACE (Gravity Recovery and Climate Experiment) and GOCE (Gravity field and steady-state Ocean Circulation Explorer) data. The combination of these datasets has been incorporated using full normal equations. The maximum degree and order of any infinite series expansion has its own benefits in delineation of smaller-scale structures. The spherical harmonic coefficients of the higher frequencies have been generated from the DTU10 terrestrial data. The gravity data generated from EIGEN6C4 has significantly lower error than the other EGM2008, EIGEN6C3 generated gravity data[19]. The effectiveness of EIGEN6C4 model data has been evaluated using several functions of the potential field and GPS/Levelling[20]. The EIGEN6C4 FAG data have been generated from http://icgem.gfz-potsdam.de/ICGEM.

Edge Enhancement Techniques

The edge detection techniques largely aim for detecting the boundaries in a digital image where a change in pixel values is observed. Geological lineaments represent geological boundaries / fracture / joint / fault/ fold or shear zones. These are exhibited by individual patterns / arrangements of the nearby features with different groups of linear patterns, tonal variation[21-24]. General, lineaments represent subsurface phenomenon[25]. Primarily, there are four types of high pass filtering techniques for edge detection, which are Canny, Sobel, Prewitt and Laplace filters[25]. The edges are obtained by convolving with the corresponding kernel either in vertical or horizontal directions. These are mostly used for shallow surface lineament detection.

In potential filed data, different derivative techniques (x, y and z directional) correlate better than its anomaly maps with geological features such as rift zones, fold belts, fractures and joints etc. These derivative techniques have been advocated for many years to delineate edges in potential field data. The horizontal derivatives (x- and y- directional) technique responds maximum, whereas the vertical derivative is zero over the vertical source edges[26-27]. Therefore, either of these techniques can be utilized in edge detection of an isolated anomaly source. But the resolution of detected edges varies when sources are non-vertical or different sources are very close or sources are at different depths. Various researchers have utilized different combinations of these horizontal and vertical derivative techniques to image the actual edge locations for both shallower and deeper sources[28-32]. These edge enhancement techniques are called balanced edge detection technique due to their nearly same amplitude response for both shallower and deeper targets. The total horizontal derivative (THD) technique is an effectively utilized classical edge detection technique[26]. The THD technique uses combination of the x- and y-directional derivatives of potential field data to delineate the edge features like faults / margins. The amplitude responses obtained from THD technique is higher for shallower sources and smaller for deeper sources. The analytical signal (AS), utilized the combination of first order vertical and horizontal derivatives. It gives maximum amplitude response over the source edge, despite of the structural dip present[28,33]. The AS technique has been broadly utilized in gravity data for enhancement of edges of causative sources[34,35]. The Theta map technique appears as a very effective tool for edge delineation in potential field data[31]. It is derived by using the cosine ratio of the THD and AS amplitude. The Theta map response for deeper sources are higher and sharper in amplitude than that of other two edge detection (THD and AS) techniques.

In order to recognize nature of the crust, trends of lineaments/fractures, different highs and lows and the source depths of anomalies over the entire area has been studied using high resolution satellite-derived EIGEN6C4 combine earth gravity model data and edge enhancement techniques. Present study deals with the multi-fold objectives which are,:- i) comparative assessment of edge enhancement technique (Theta map) over classical edge detection techniques (AS and THD) for delineation of edge features of various depth sources, ii) establishing the utilization of uniform EIGEN6C4 FAG data for delineation of the structural features specially over the remote and inaccessible offshore regions, iii) recognition of the major anomalous structural and tectonic elements and their trends over the Laxmi ridge and its surroundings. The major deliverables of this work are mapping of the major structural features

$$Theta = \cos^{-1}\left(\frac{THD}{AS}\right)$$

resulted due to the stress variations in various geological periods, identification of the anomalous zones and estimation of anomaly source depths over the study area especially for hydrocarbon exploration.

Methodology

Any potential field observed in one plane may be continued mathematically upwards or downwards to any other plane if there are no anomalous mass between these two planes. In this case the potential function will satisfy the Laplace's equation. Upward continuation has been utilized in potential field data to identify the characteristics of the long wavelength (regional) anomaly distribution. Continuation operator in frequency domain can be represented as below:[36]

$$\sum_{f=-n/2}^{+n/2} \exp[2\pi i\, f(z_o - z_1)/\lambda]$$

where z_0 is initial plane and z_1 is the plane at which gravity anomaly is to be computed Z is positive in the downward direction and negative in the upward direction.

Edge detection techniques are mostly functions using combination of different gradients of potential field data. One of the most common approaches is total horizontal derivative (THD). It is computed using the following equation[26]:

$$THD = \sqrt{\left(\frac{\partial g}{\partial x}\right)^2 + \left(\frac{\partial g}{\partial y}\right)^2}$$

Analytic signal (AS) amplitude is computed using the combination of both vertical and horizontal derivatives. The AS amplitude is computed using the equation given here under[28,33]:

$$AS = \sqrt{\left(\frac{\partial g}{\partial x}\right)^2 + \left(\frac{\partial g}{\partial y}\right)^2 + \left(\frac{\partial g}{\partial z}\right)^2}$$

where, $\frac{\partial g}{\partial x}, \frac{\partial g}{\partial y}, \frac{\partial g}{\partial z}$ are the horizontal (x and y directions) and vertical derivative of the gravity anomaly, respectively.

The theta (θ) map technique is defined as the normalization of the THD amplitude by the AS amplitude[31].

Observations from the synthetic models

Initially, synthetic model of prismatic sources with two different depth have been generated to evaluate the effectiveness of the θ map technique over THD and AS techniques. At the source margins, THD and AS techniques show maximum amplitudes whereas, theta map technique shows a minimum. A considerable amount of difference also observed in their amplitudes and edge locations of the source anomalies. The physical properties of the presently adopted 2-D model are mentioned in Table 1.

The generated gravity anomaly (GA) map shown in (Fig. 2b), has been enhanced using THD, AS and Theta map techniques for the given model parameters. Their responses are shown in (Figs. 2b-e), respectively. From (Fig. 2c), it is observed that the THD responses from shallower sources are larger in amplitude and smaller for deeper sources. However, the THD anomalies are broader in nature so that delineated edges may offset from actual edges for both sources. From (Fig. 2d), it is observed that AS responses for shallower source are larger in amplitude, while smaller for deeper sources. The observed AS amplitude response from shallower source is sharper enough to delineate the correct source edge. But, in case of deeper source, there is deviation from actual edges. Figure 2e demonstrates that theta map anomaly responses are larger, sharper and balanced for both shallow and deeper sources with only difference that deeper anomaly response is bit coarser than that of shallower. It is observed that the edges delineated using theta map shows minimal deviation from its actual source edges. It is observed that theta map technique is more suitable to delineate the edges of the sources with different depths.

Table-1 — Physical parameters of the synthetic gravity anomaly models for the two vertical prisms

Physical parameters	Prism 1	Prism 2
Depth to the center (m)	20	33
Density contrast (kg/m^3)	0.5×10^3	0.5×10^3
Horizontal extension (m)	8	10
Top (m)	17	30
Bottom (m)	23	36

Sharpening in gravity response is a result due to removal of effects of nearby anomalies, which are generated through surrounding rather than the actual sources. The deviation from the actual edges might be due to non-vertical sources or very closely situated objects or superposition of sources or very complex geological structures and sometimes due to incompetency of edge delineation techniques etc. A comparative study of 12 different edge detection techniques infers that there is no single edge enhancement technique which bears all desirable attributes for displaying accurate edge locations, simultaneously for various source of characteristics[37]. But, the problem could be resolved to a greater extent using balanced edge detection techniques, like the theta map which provide larger and relatively sharper anomaly responses than those of conventional derivative techniques for both shallow and deeper sources. In the present evaluation, theta map techniques shows much better resemblance in delineation of true source edge locations for all depth seated objects.

Application of EIGEN6C4 FAG data over the Laxmi ridge

The effects of past geological phenomenon and its footprints can be observed in different gravity anomaly maps[38-41]. To have a better understanding of the nature of crust over the study area, it is crucial to understand the past tectonic activities, course of structural features and evolution history of the area using recent high-resolution satellite-derived gravity data and suitable techniques[10,11,41]. These studies become more informative especially in remote and inaccessible regions like offshore. Some researchers have utilized the high resolution potential field

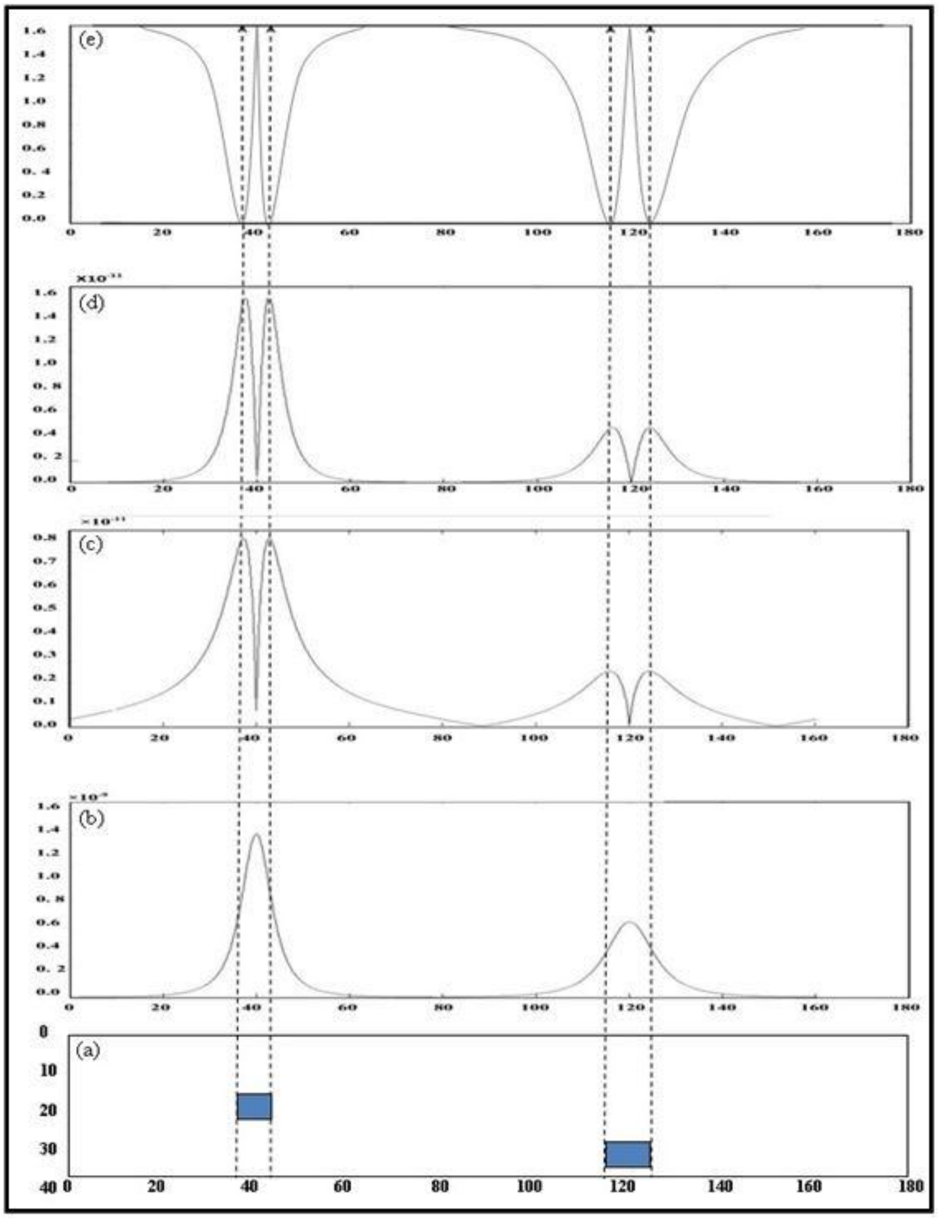

Fig. 2 (a) — Synthetic model of two vertical prisms at depths of 25 m and 33 m, (b) Gravity anomaly (GA) response, (c) Total horizontal derivative of GA, (d) Analytical signal amplitude of GA and (e) Theta response of GA.

data[11-13,16-18,41]. Using effective techniques they successfully delineated the edge features, anomalous zones and trends of major lineaments in various parts of the India[16-18] and Indian Ocean[11-13,41] .

Study using edge enhancement techniques

The free-air gravity (FAG) anomaly map generated using EIGEN6C4 over the study area is shown in (Fig. 3a). The FAG generated using EIGEN6C4 has been validated (Fig. 3b) by comparison with -ship-borne FAG data along RE-11 by Krishna et al.[10]. The comparative study indicates that correlation coefficient and covariance between the two data sets along the profile are about 0.94 and 94.2 mgal^2. It reveals that FAG generated using EIGEN6C4 highly correlated and could be used for detail analysis. Laxmi ridge is delineated well with prominent negative gravity of about -53 mGal and -56 mGal in EIGEN6C4 generated and ship-borne data, respectively.

The residual gravity anomaly map with different cut-off wavelengths of 50 km, 100 km, 150 km and 200 km have been generated and qualitatively examined. Residual gravity anomaly map with cut-off wavelength of 50 km and 100 km are shown in Figs. 4a&b, respectively. It is observed that the residual map (Fig. 4b) with cut-off wavelength of 50 km enhances mostly shallower features whereas, the residual anomaly map (Fig. 4b) with cut-off wavelength of 100 km delineates relatively medium to longer wavelength features. Considering model crustal structure across Laxmi basin, Panikkar ridge, Laxmi ridge and eastern Arabian Sea by Krishna et al.[10], the residual gravity anomaly map with cut-off wavelength of 100 km has been utilized for further understanding of the structures of Laxmi ridge and surroundings. Several high and low zones are observed in the residual anomaly map (Fig. 4a). Ridge extension from its NW-SE trend to WNW–ESE trend has been demarcated excellently (Fig. 4b).

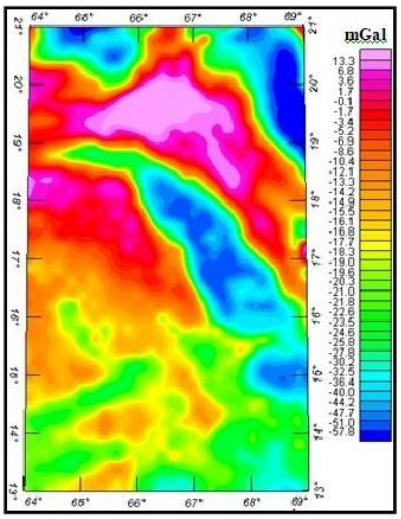

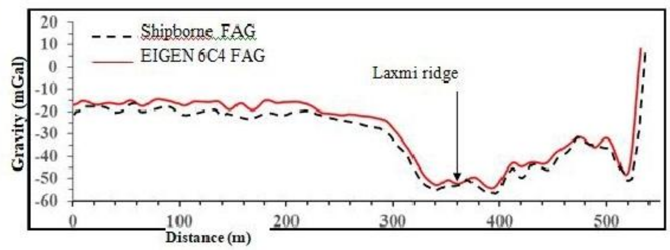

Fig. 3a — Unfiltered EIGEN6C4 free-air gravity (FAG) anomaly map over the Laxmi ridge and its surroundings; Fig. 3b — Comparison of Ship FAG and EIGEN 6C4 FAG data along RE-11 of Krishna et al.[10]. Laxmi ridge is delineated with prominent negative gravity.

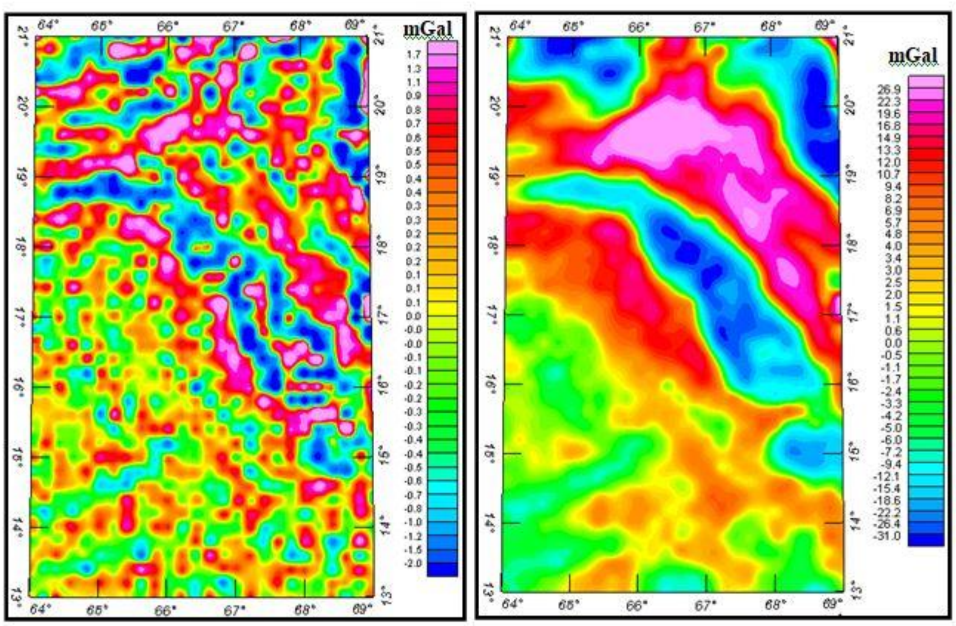

Fig. 4 — Residual of EIGEN6C4 free-air gravity (FAG) anomaly map upto b) 50km and b) 100km over the Laxmi ridge and its surroundings.

The residual gravity anomaly with cut-off wavelength of 100 km has been enhanced using THD, AS and Theta techniques. Application of edge enhancement techniques over the residual gravity anomaly provides better image for delineation of the subsurface features corresponding to different depths. The lineaments are delineated from THD, AS and θ anomaly maps based on different anomaly patterns over the entire region and these are shown in (Figs. 5a,b,c), respectively. It is observed from (Fig. 5a) that the THD technique delineates edges from shallower objects but failed to delineate edges from deeper objects. The comparative/qualitative evaluation of THD, AS and Theta map techniques for lineament extraction have been carried out based on the analysis of synoptic Rose diagrams. Generated synoptic Rose diagram based on lineaments trends infers that THD technique (Fig. 6a) delineates the major lineaments in NW-SE direction followed by NE-SW, E-W, and N-S directions. In general, the lineaments delineated at right side of the Laxmi ridge have similar trends as the lineament trends in the whole area (Figs. 6a-c). Though, prominent random lineament trends are observed on the left side than that of the right side (Figs. 6b-c). The NW-SE trend is very much prominent in right side (Fig. 6c). Figure 5b illustrates that the AS technique delineates edges from shallower and medium depth objects but could not able to delineate edges from deeper objects. Generated synoptic rose diagram based on lineaments trends infers that AS technique (Fig. 7a) delineates the major lineaments in the N-S direction followed by NE-SW, NW-SE and E-W directions, respectively. In general, lineaments on both right and left side of

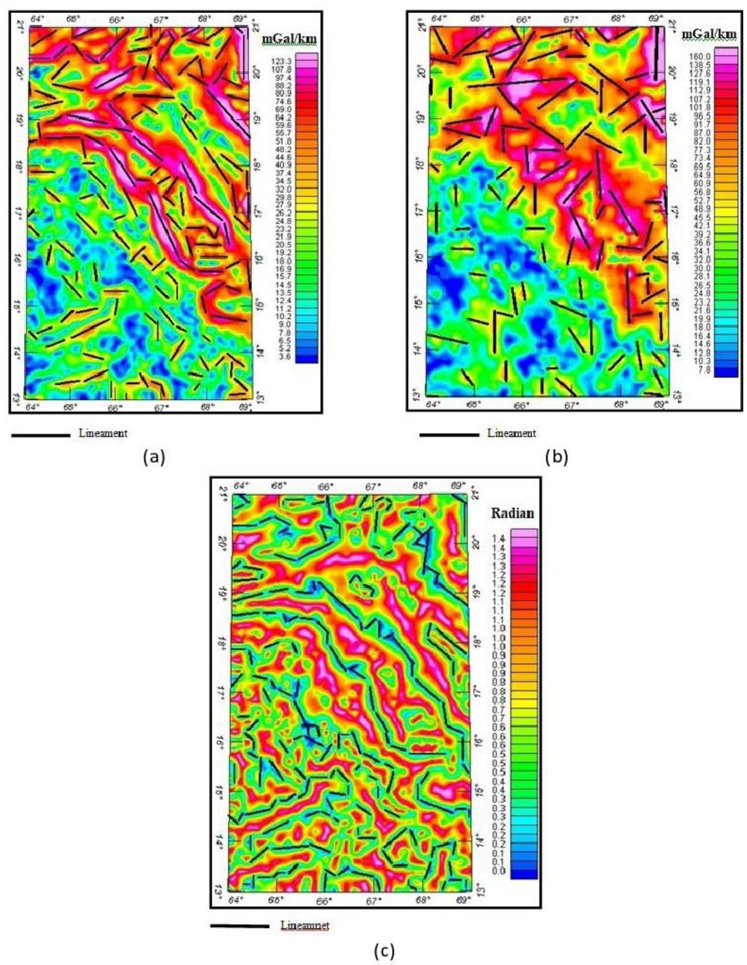

Fig. 5a — Total Horizontal Derivative (THD) map of the 100km residual FAG anomaly over the Laxmi ridge and in its vicinity. These lineaments (THD linea) have been recognized based on distinct anomalous THD characteristics; Fig. 5b — Analytical Signal (AS) map of the 100km residual FAG anomaly over the Laxmi ridge and in its vicinity. These lineaments (AS linea) have been recognized based on distinct anomalous AS characteristics; Fig. 5c — Theta map of the 100km residual FAG anomaly over the Laxmi ridge and in its vicinity. These lineaments (Theta linea) have been recognized based on distinct anomalous Theta anomaly characteristics.

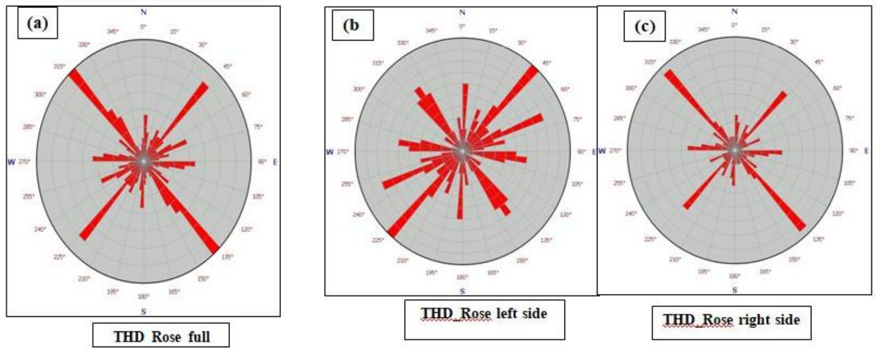

Fig. 6 — Synoptic Rose diagram of (a) THD Rose full area, (b) THD Rose left side area and (c) THD Rose right side area lineaments representing their trends over the study area.

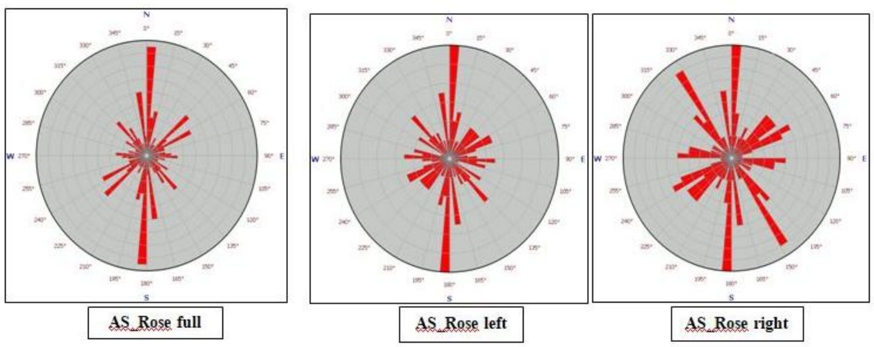

Fig. 7 — Synoptic Rose diagram of (a) AS Rose full area, (b) AS Rose left side area and (c) AS Rose right side area lineaments representing their trends over the study area.

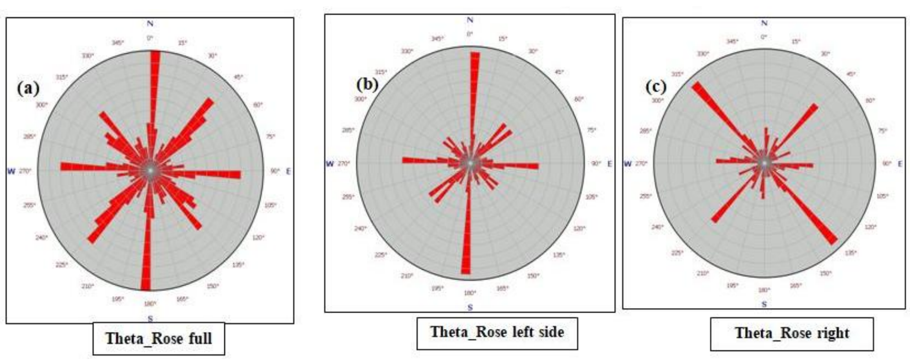

Fig. 8 — Synoptic Rose diagram of (a) Theta Rose full area, (b) Theta Rose left side of ridge axis and (c) Theta Rose right side of ridge axis lineaments representing their trends over study area.

study area have similar trends (Figs. 7b-c) as the lineament trends in the whole area (Fig.7a). However, the NW-SE trend is prominent in right side (Fig.7c) whereas, (Fig. 5c) illustrates that the Theta map technique delineates all the edges including the shallower, medium and deeper objects, more accurately than the THD and AS techniques. Generated synoptic Rose diagram infers that the Theta technique (Fig. 8a) delineates the major lineaments in N-S direction followed by NE-SW, E-Wand NW-SE directions. Only limited numbers of N-S trending lineaments could be observed in the right side of the study area, unlike the left side and the whole area (Figs. 8b-c). Theta map technique delineates deeper lineaments better than THD and AS technique. Previous study indicates the major lineament trends in only NW-SE, NNW-SSE and NE-SW directions[42]. Interestingly, all the previously reported structural trends have been delineated and some additional lineament trends have also been delineated in the present study. It is observed that using all three techniques, the NW-SE trend is the prominent lineament trend followed by NE-SW in right side of the ridge (Figs. 6-8) whereas, random nature of lineament trends are observed on the left side than that of the right side.

Study using upward continuation

The upward continued gravity anomalies have been generated at heights of 20 km, 40 km, 60 km, 90 km and 150 km, respectively for understanding the source depth of anomalies beneath the ridge. These upward continued regional maps have been further enhanced with the theta technique to closely observe the change in anomaly variation corresponding to ridge extension (Figs. 9a-e). Anomaly map (Fig. 9a) generated at height 20 km shows ridge anomaly trend similar to gravity anomaly with some reduction in gravity value. It suggests that source anomaly depth under the ridge is below the upper crust. The NNW-SSE trending part of the ridge starts widening and gravity values start reducing at higher rate in the upward continued maps generated at heights 40 and 60 km (Fig. 9b-c). At height 90 km, the NNW-SSE trending part of the ridge get disappeared and NW-SE trending part of the ridge anomaly still poses a considerable amount of gravity value (Fig. 9d). It suggests that the ridge density anomaly has some contribution from deeper crust and mantle. Upward continuated map at height 150 km (Fig. 9e) reveals that the NW-SE trending part of the ridge anomalies nearly vanished and almost shrink to a point object at around 67.8^0E and 16.6^0N. From above observations, our study suggests that the ridge is constituted of low density mantle materials covered with recent sediments brought by Indian sub-continental rivers. The right side (NW-SE trending part) of the ridge crust is of the continental nature, whereas left side (NNW-SSE trending part) is of the oceanic nature.

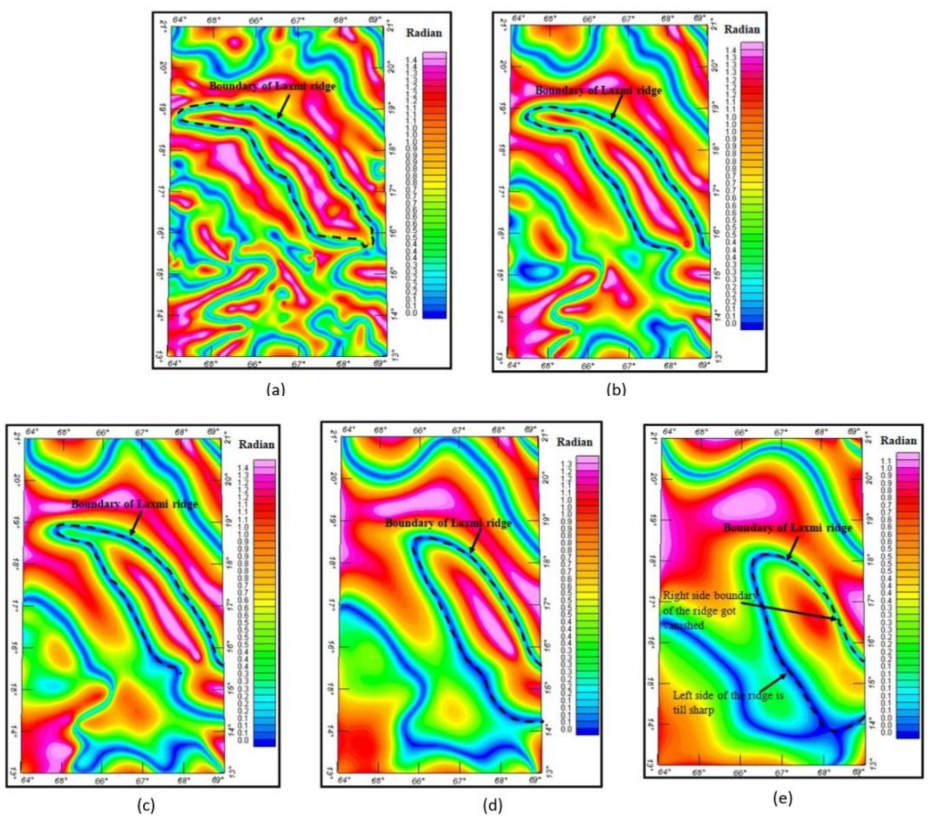

Fig. 9a — Theta enhanced map of the upward continued gravity anomaly at height of 20 km over the study area. The result shows that the most of the Laxmi ridge gravity anomaly is contributed by crustal materials present underneath in the area; (b) Theta enhanced map of the upward continued gravity anomaly at height of 40 km over the study area. The NNW-SSE trending part of the ridge anomaly starts widening and diminishing (c) Theta enhanced map of the upward continued gravity anomaly at height of 60 km over the study area. Most of the NNW-SSE trending part of ridge anomaly is vanished (d) Theta enhanced map of the upward continued gravity anomaly at height of 90 km over the study area. NNW-SSE trending part of ridge anomaly is completely vanished and NW-SE part of the ridge also decreasing. (e)heta enhanced map of the upward continued gravity anomaly at height of 150 km over the study area. Almost the entire ridge anomaly got vanished and turn into about a point source at around 67.8^0E and 16.6^0N .

Some prominent gravity highs and lows are also identified over the entire study area, which were not apparent in previous studies. It is observed that shallower and deeper structures have different trends. The deeper features have major trends in NW-SE and NE-SW directions, whereas shallower features follow the trends in almost all directions, randomly. There are some controversies about the crustal framework below the Laxmi ridge in spite of various geophysical studies. Some scientists concluded that in the right side of the study area, the ridge acts as transitional boundary from the rifted crust, whereas it is oceanic in nature on the left side[4,6,43,44]. However, some other scientist concluded that the crusts below the ridge are oceanic in nature only[5,45,46]. The previous study showed that the southward extension of the seafloor expression of the NW-SE_trending part of the Laxmi ridge seems to abruptly terminated against an oceanic crust, which contains magnetic lineation in E-W direction[47]. Present study reveals that the edge enhancement techniques provide valuable information for geologists and petroleum engineers to outline the horizontal location of geological sources and other tectonic and geological features. A series of gravity low zones identified in the residual anomaly map may be related to deposition of low density recent sediments or down bending of crust. Present study also supplemented the previous studies, which states that gravity low (negative) along the Laxmi ridge is due to down-bending at the lower crust, and subsequent flow of excessive magmatic constituents underneath the ridge[36]. Due to these reasons, in spite of being prominently structural high, the Laxmi ridge portrays negative FAG anomaly.

Conclusion

The comparative study of EIGEN6C4 FAG data and ship-borne FAG data indicate correlation coefficient 0.94 and proves the suitability of EIGEN6C4 FAG data for study of structure and tectonic of Laxmi ridge and surroundings. The ability to delineate the shallow and deeper features makes the Theta map technique most suitable for edge enhancement. Previous study depicts that the major trends of the lineaments are only in NW-SE, NNW-SSE and NE-SW directions in the area[42]. It is very fascinating that the entire observed structural features match well with the previous studies[42] and some additional lineament trends have also been delineated in the present study. Major lineaments occurring over the region are in N-S, NE-SW and NW-SE directions followed by E-W, ENE-WSW and NNW-SSE directions. The NW-SE trend is the prominent lineament trend followed by NE-SW in right side of ridge. However, random nature of lineaments trends is observed in the left side than that of the right side of the study area. The delineated lineaments and its orientations are the results of rifting and break-up of India, Madagascar and Seychelles since the mid-Cretaceous, which control the structural pattern of western India as well as its offshore region. The upward continued generated gravity anomaly maps at heights 20 km, 40 km, 60 km, 90 km and 150 km showed that the right side area of the ridge crust have continental source of crust, whereas left side crust is oceanic in nature.

Acknowledgement

Authors are highly indebted to the reviewers for the detail revision and the valuable suggestions for improving manuscript. We thank International Centre for Global Earth Models (ICGEM) for providing EIGEN6C4 gravity data. We thank British Oceanographic data centre (BODC) for providing gridded bathymetry data (GEBCO). We also thank the Director, IIT(ISM), and the Head, Dept. of App. Geophysics, IIT(ISM), Dhanbad for their keen interest in this study.

References

1 Norton I O & Sclater J G, A model for the evolution of the Indian Ocean and the breakup of Gondwanaland, *J. Geophys. Res.*, (1979) Vol. 84, pp. 6803–6830.

2 Courtillot V, Besse J, Vandamme D, Montigny R, Jaeger J J & Capetta, H, Deccan flood basalts at the Cretaceous/ Tertiary boundary, *Earth Planet. Sci. Lett.*, (1986) 80: 361-374. doi: 10.1016/0012-821X(86)90118-4.

3 White R & McKenzie D, Magmatism at rift zones–The generation of volcanic continental margins and flood basalts, *J. Geophys. Res.*, (1989) 94, 7685–7729.

4 Miles P R & Roest W R, Earliest sea-floor spreading magnetic anomalies in the north Arabian Sea and the ocean–continent transition, *Geophys. J. Int.*, (1993) 115 1025–1031.

5 Malod J A, Droz L, Kemal B M & Patriat P, Early spreading and continental to oceanic basement transition beneath the Indus deep-sea fan: Northeastern Arabian Sea, *Mar. Geol.*, (1997) 141 221–235. 114:B03102 doi: 10.1029/ 2008JB005808.

6 Naini B R & Talwani M, Structural framework and the evolutionary history of the continental margin of western India. In: Walkins JS, Drake CL (eds) Studies in continental margin geology, *Am. Assoc. Pet. Geol. Memoir.*, (1982) 34, pp 167–191.

7 Biswas S K, Regional tectonic framework, structure and evolution of the western marginal basins of India, *Tectonophy.*, (1987) 135:307–327.

8 GopalaRao D, Ramana M V, Bhattacharya G C, SubbaRaju L V, KameshRaju K A & Ramprasad T, Marine geophysical studies along a transect across the continental margin of Bombay coast, west of India, *In: Oceanography of the Indian Ocean (ed.) B N Desai, IBH Publications*, New Delhi, (1992) pp. 493–501

9 Krishna K S, Murty G P S, Srinivas K & GopalaRao D, Magnetic studies over the northern extension of the Prathap Ridge complex, eastern Arabian Sea, *Geo-Mar., Lett.*, (1992) 12, 7-13.

10 Krishna K S, Gopala Rao D & Sar D, Nature of the crust in the Laxmi Basin (14^o – 20^oN), western continental margin of India, *Tectonics*, (2006), 25, TC1006, 18 p.

11 Majumdar T J, Mohanty K K & Srivastava A K, On the utilization of ERS-1 altimeter data for offshore oil exploration, *Int. J. Remote Sens.*, (1998) 19(10):1953-1968.

12 Pal S K, Narayan S, Majumdar T J & Kumar U, Structural mapping over the 85°E Ridge and surroundings using EIGEN6C4 high-resolution global combined gravity field model: an integrated approach, *Mar. Geophy. Res.*, (2016) 37: 159. doi:10.1007/s11001-016-9274-3.

13 Satya Narayan, Sahoo S D, Pal S K, Kumar U, Pathak V K, Majumdar T J & Chouhan A, Delineation of structural features over a part of the Bay of Bengal using total and balanced horizontal derivative techniques, *Geocarto Int.*, (2016) DOI: 10.1080/10106049.2016.1140823

14 Shin Y H, Xu H, Braitenberg C, Fang J & Wang Y M, Moho undulations beneath Tibet from GRACE-integrated gravity data, *Geophys. J. Inter.*, (2007) 170:971–985.

15 Shako R, Förste C, Abrikosov O, Bruinsma S L, Marty J C, Lemoine J M, Flechtner F, Neumayer K H & Dahle C, EIGEN-6C: A high resolution Global Gravity Combination Model iIncluding GOCE data; *In: Flechtner F, et al. (ed.) Observation of the System Earth from Space–CHAMP GRACE GOCE and future missions Advanced Technologies in Earth Sciences*, (2014) DOI: 10.1007/978-3-642-32135-1_20 Springer-Verlag Berlin.

16 Jitendra Vaish & S K Pal, Geological mapping of Jharia Coalfield, India using GRACE EGM2008 gravity data: a vertical derivative approach, *Geocarto Int.*, (2015) 30(4): 388-401

17 Pal S K & Majumdar T J, Geological appraisal over the Singhbhum-Orissa Craton, India using GOCE, EIGEN6-C2 and in-situ gravity data. *Int. J. Applied Earth Observ. Geoinfo.*, (2015) 35, 96-119.

18 Pal S K, Majumdar T J, Pathak V K, Satya Narayan, Ujjawal Kumar & Om Prakash Goswami, Utilization of high resolution EGM2008 gravity data for geological exploration over the Singhbhum-Orissa Craton, India. *Geocarto Int.* (2016), 31(7) 783-802. DOI:10.1080/ 10106049.2015.1076064,

19 Förste C, Bruinsma S, Abrykosov O, Lemoine J M, The latest combined global gravity field model including GOCE data up to degree and order 2190 of GFZ Potsdam and GRGS Toulouse, *5th GOCE User Workshop Paris*, (2014) 25–28 Nov. 2014. http://icgem.gfz-potsdam.de

20 Klokocnik J, Kostelecky J, Bucha B A & Foerste C, Evaluation of EIGEN-6C4 by means of various functions of the gravity potential, and by GPS/Leveling, *Geophy. Res. Abst. EGU General Assembly*, (2015) Vol. 17, EGU2015-3910.

21 Pal S K, Bhattacharya A K, & Majumdar T J, Geological interpretation from Bouguer gravity data over the Singhbhum-Orissa Craton and its surroundings: A GIS approach. *J. Indian Geophys. Union* (2006) 10(4) 313-325.

22 Pal S K, Majumdar T J, Bhattacharya A K, Extraction of linear and anomalous features using ERS SAR data over Singhbhum Shear Zone, Jharkhand using fast Fourier transform. *Int. J. of Rem. Sens.* (2006) 27(20) 4513–4528

23 Pal S K, Majumdar T J, Bhattacharya A K, Usage of ERS SAR data over the Singhbhum shear zone, India for structural mapping and tectonic studies, *Geocarto Int.* (2007) 22: 285–295. DOI:10.1080/10106040701337642.

24 Pal S K, Majumdar T J, Bhattacharya A K, ERS-2 SAR and IRS-1C LISS III data fusion: a PCA approach to improve remote sensing based geological interpretation, *ISPRS. J. Photogramm Rem. Sens.* (2007) 61:281–297.

25 Sabins Jr FF, Remote Sensing: Principles and Interpretation, *W.H. Freeman & Co., New York, USA* (1997) 494 pp.

26 Cordell L & Grauch V J S, Mapping basement magnetization zones from aeromagnetic data in the San Juan basin, New Mexico, In: W.J. Hinze (Ed.), The Utility of Regional Gravity and Magnetic Anomaly Maps, *Society of Explor. Geophys.*, (1985) pp. 181–197.

27 Telford W M, Geldart L P & Sheriff R E, Applied Geophysics. *Cambridge University Press, New York, USA*, (1990) 770 p.

28 Roest W R, Verhoef J & Pilkington M, Magnetic interpretation using the 3-D analytic signal, *Geophys.*, (1992) 57:116–125.

29 Hsu S K, Sibuettand J C & Shyu C T, High-resolution detection of geologic boundaries from potential-field anomalies: an enhanced analytic signal technique, *Geophys.*, (1996) 61:373–386.

30 Verduzco B, Fairhead J D Green C M & Mackenzie C, New insights into magnetic derivatives for structural mapping, *Lead Edge*, (2004) 23, 116–119.

31 Wijns C, Perez C & Kowalczyk P, Theta map: edge detection in magnetic data, *Geophys*, (2005) 70:L39–L43.

32 Cooper G R J. & Cowan D R, Enhancing potential field data using filters based on the local phase, *computer & geosci.*, (2006) 32, 1585-1591. http://dx.doi.org/10.1016/ j.cageo. 2006.02.0

33 Nabighian M N, The analytic signal of two-dimensional magnetic bodies with polygonal cross-section: Its properties and use for automated anomaly interpretation, *Geophys*, (1972) 37: 507–517.

34 Green R & Stanley J M, Application of a Hilbert transforms method to the interpretation of surface-vehicle magnetic data, *Geophys. Pros.*, (1975) 23:18–27.

35 Klingele E E, Marson I & Kahle H G, Automatic interpretation of gravity gradiometric data in two dimensions: vertical gradient, *Geophys. Pros.*, (1991) 39, 407–434.

36 Blakely R, Potential Theory in Gravity and Magnetic Applications, *Cambridge University Press, Cambridge, U.K.*, (1996) pp.435.

37 Pilkington M & Keating P B, The utility of potential field enhancements for remote predictive mapping, *Can. J. Remote Sens.*, (2009) 35(Suppl. 1):S1–S11.

38 Watts A B & Fairhead J D, A process oriented approach to modelling the gravity signature of continental margins, *Lead Edge*, (1999) 18:258–263.

39 Tiberti M M, Orlando L, DiBucci D, Bernabini M & Parotto M, Regional gravity anomaly map and crustal model of the Central–Southern Apennines (Italy), *J. Geodyn.*, (2005) 40 73–91.

40 Krishna K S, Michael L, Bhattacharyya R & Majumdar T J, Geoid and gravity anomaly data of conjugate regions of Bay of Bengal and Enderby Basin: New constraints on breakup and early spreading history between India and Antarctica, *J. Geophys. Res.*, (2009) https://doi.org/10.1029/ 2008JB005808.

41 Kumar U, Pal S K, Sahoo S D, Narayan S, Saurav, Mondal S, Gunguli S S, Lineament mapping over Sir Creek offshore and its surroundings using high resolution EGM2008 Gravity data: An integrated derivative approach, *J. Geol. Soc. India* (2018) 91(6) 671-678.

42 Majumdar T J & Bhattacharyya R, Bathymetry prediction model from high-resolution satellite gravity as applied over a part of the eastern Indian offshore, *Curr. Sci.*, (2005) 89(10): 1754-1759.

43 Kolla V & Coumes F, Extension of structural and tectonic trends from the Indian subcontinent into the eastern Arabian Sea, *Mar. Petrol. Geol.*, (1990) 7 188–196.

44 Pandey O P, Agarwal P K & Negi J G, Lithospheric structure beneath Laxmi Ridge and late Cretaceous geodynamic events, *Geo. Mar. Lett.*, (1995) 15 85–91.

45 Bhattacharya G C, Chaubey A K, Murthy G P S, Srinivas K, Sarma K V L N S, Subrahmanyam V & Krishna K S, Evidence for seafloor spreading in the Laxmi Basin, northeastern Arabian Sea, *Earth Planet Sci. Lett.*, (1994) 125 211–220.

46 Chaubey A K, Bhattacharya G C, Murthy G P S, Srinivas K, Ramprasad T & GopalaRao D, Early Tertiary seafloor spreading magnetic anomalies and paleo-propogators in the northern Arabian Sea, *Earth Planet Sci. Lett.*, (1998) 154 41–52.

47 Bhattacharya G C & Chaubey A K, Western Indian Ocean a glimpse of the Tectonic Scenario. In: *The Indian Ocean-a perspective; Edited by R. Sen Gupta R and E. Desa, Oxford & IBH Publishers, New Delhi*, (2001) pp. 691–729.